THE JOURNAL OF BIOLOGICAL CHEMISTRY VOL. 287, NO. 48, pp. 40161–40172, November 23, 2012

Kuppfer Cells Trigger Nonalcoholic Steatohepatitis Development in Diet-induced Mouse Model through Tumor Necrosis Factor-α Production*[S]

Received for publication, September 6, 2012, and in revised form, October 4, 2012 Published, JBC Papers in Press, October 12, 2012, DOI 10.1074/jbc.M112.417014

Annie-Carole Tosello-Trampont[‡], Susan G. Landes[‡], Virginia Nguyen[‡], Tatiana I. Novobrantseva[§], and Young S. Hahn[‡¶1]

From the [‡]Beirne Carter Center for Immunology Research, [¶]Department of Microbiology, University of Virginia, Charlottesville, Virginia 22908 and [§]Alnylam Pharmaceuticals, Cambridge, Massachusetts 02142

Background: The mechanisms triggering nonalcoholic steatohepatitis (NASH) remain poorly defined.
Results: Kupffer cells are the first responding cells to hepatocyte injuries, leading to TNFα production, chemokine induction, and monocyte recruitment. The silencing of TNFα in myeloid cells reduces NASH progression.
Conclusion: Increase of TNFα-producing Kupffer cells is crucial for triggering NASH via monocyte recruitment.
Significance: Myeloid cells-targeted silencing of TNFα might be a tenable therapeutic approach.

Nonalcoholic steatohepatitis (NASH), characterized by lipid deposits within hepatocytes (steatosis), is associated with hepatic injury and inflammation and leads to the development of fibrosis, cirrhosis, and hepatocarcinoma. However, the pathogenic mechanism of NASH is not well understood. To determine the role of distinct innate myeloid subsets in the development of NASH, we examined the contribution of liver resident macrophages (*i.e.* Kupffer cells) and blood-derived monocytes in triggering liver inflammation and hepatic damage. Employing a murine model of NASH, we discovered a previously unappreciated role for TNFα and Kupffer cells in the initiation and progression of NASH. Sequential depletion of Kupffer cells reduced the incidence of liver injury, steatosis, and proinflammatory monocyte infiltration. Furthermore, our data show a differential contribution of Kupffer cells and blood monocytes during the development of NASH; Kupffer cells increased their production of TNFα, followed by infiltration of CD11b^{int}Ly6C^{hi} monocytes, 2 and 10 days, respectively, after starting the methionine/choline-deficient (MCD) diet. Importantly, targeted knockdown of TNFα expression in myeloid cells decreased the incidence of NASH development by decreasing steatosis, liver damage, monocyte infiltration, and the production of inflammatory chemokines. Our findings suggest that the increase of TNFα-producing Kupffer cells in the liver is crucial for the early phase of NASH development by promoting blood monocyte infiltration through the production of IP-10 and MCP-1.

Nonalcoholic steatohepatitis (NASH)[2] is a metabolic liver disease leading to progressive fibrosis, cirrhosis, and liver cancer (1). No medical treatment has been established yet to treat NASH patients. The histological features of NASH are characterized by the accumulation of lipid within hepatocytes (steatosis) accompanied by hepatic injury and inflammation. The cellular/molecular biomarkers differentiating benign steatosis and NASH remain poorly defined. A better understanding of NASH pathogenesis is essential for the development of novel effective therapies to limit hepatic injury and inflammation.

A "two-hit model" has been postulated as a potential mechanism responsible for NASH pathogenesis, in which the first "hit" is provided by metabolic syndrome (steatosis), and the second hit, which can include oxidative stress, inflammation, or gut-derived endotoxins, propels the progression from steatosis to steatohepatitis. However, recent studies have indicated that inflammation may also precede or develop in parallel to hepatic steatosis (2). Thus, extrahepatic inflammation may affect liver function via secreted soluble factors leading to the activation of innate immunity and facilitating progression of hepatic steatosis and inflammation. Innate immune cells (such as blood-derived monocytes and liver resident macrophages, termed Kupffer cells), are likely to play a pivotal role in responding to inflammation and metabolic stresses by orchestrating local immune responses through the secretion of cytokines and chemokines.

Recently, MCP-1 levels appear to be increased in NASH patients and in diet-induced NASH models (3–5). MCP-1 is a major chemokine responsible for the recruitment of leukocytes into the liver during hepatic inflammation through the activation of CCR2 receptor displayed on inflammatory cells such as Ly6C^{hi} monocytes. The absence or the inhibition of CCR2 reduced the development of obesity, adipose tissue, and hepatic inflammation as well as monocyte/macrophage accumulation in diet-induced NASH (5–7). A recent study reported that infiltration of Ly6C^{+} bone marrow-derived macrophages promotes NASH after 22 weeks of diet, at which point the disease is well established (5). Moreover, the distinct role of infiltrated monocytes and resident macrophages in NASH development has not been defined.

* This work was supported in part by National Institutes of Health Grants R01DK063222 and U19AI083024 (to Y. S. H.)
[S] This article contains supplemental Figs. S1–S3.
[1] To whom correspondence should be addressed: P. O. Box 801386, Charlottesville, VA 22908-1386. Tel.: 434-924-1155; Fax: 434-924-1221; E-mail: ysh5e@cms.mail.virginia.edu.
[2] The abbreviations used are: NASH, nonalcoholic steatohepatitis; MCD, methionine/choline deficient; qPCR, quantitative PCR; TIMP-1, tissue inhibitor of metalloproteinase-1; MFI, mean fluorescent intensity; ALT, alanine asminotransferase; HCV, hepatitis C virus; CT, control.

To determine the distinct role of inflammatory monocytes and resident liver macrophages in NASH and to identify crucial inflammatory mediators involved in the initiation and progression of the disease, we employed the methionine/choline-deficient (MCD) diet as a murine model of NASH. This diet affects the transport and storage of triglycerides leading to the accumulation of intrahepatic lipids (8). Although most studies with diet-induced murine NASH models were done when the disease was already well established (after 4 to 22 weeks of diet) (5, 9–11), our study focused on an early developmental stage of NASH, after only 2 and 10 days of feeding. By examining the disease at a very early stage, we were able to determine the cellular and soluble mediators involved in triggering NASH. After 10 days on the MCD diet, we are able to observe characteristics of NASH pathogenesis such as steatosis, liver inflammation, and monocyte infiltration. Our data suggest that $CD11b^+Ly6C^+$ myeloid cells, which include both Kupffer cells and monocytes, contribute to the progression of NASH development, although with different kinetics. Moreover, Kupffer cells are critical for the production of TNFα and recruitment of monocytes that in turn leads to further liver damage and disease progression. The silencing of TNFα in targeted myeloid cells prevents the infiltration of monocytes by blocking the production of IP-10 and MCP-1, lessening the progression of NASH. Thus, our results suggest that the silencing of TNFα expression in myeloid cells could be a novel therapeutic approach to treat NASH patients.

EXPERIMENTAL PROCEDURES

Mice and Diets—All experiments were performed either on 6- or 10-week-old female C57BL/6 mice (Taconic Farms). Mice were fed a MCD diet (TD.90262, Harlan Laboratories) and a control diet (TD.94149) for 2, 6, 8, or 10 days. All mice were kept in a pathogen-free facility at the University of Virginia, and were handled according to mouse protocols approved by the University or Virginia Animal Care and Use Committee.

Serum Alanine Aminotransferase (ALT) Activity—Blood was collected by cardiac puncture on anesthetized mice and transferred into BD microtainer Serum Separator Tubes (BD Biosciences). ALT activity were detected using an ALT (SGPT) kit (Pointe Scientific, Inc.).

Histological Assays (H&E, Oil Red O, and Quantification)—PBS-perfused liver tissues were fixed overnight in 10% formalin, and then embedded in paraffin. Sections of 3–4 μm were stained with conventional hematoxylin and eosin (H&E) stains. Oil Red O staining of liver sections was performed on 4-h formalin-fixed, and overnight sucrose-protected tissues at 4 °C, and then on OCT-embedded frozen tissues. Cryostat-cut 5-μm thick tissue sections were stained with Oil Red O solution (Electron Microscopy Sciences). Tissue images were captured on Olympus BX51 high magnification microscopy at the Advanced Microscopy Facility at the University of Virginia. Scaling of each image was done with micrometer slide. Images were analyzed with Zeiss axiovision software to quantify the area in μm^2 of Oil Red O-stained vesicles.

Immunofluorescent Assays—Frozen tissues section were fixed, rehydrated in PBS, and blocked with PBS containing 5% normal goat serum for 30 min at room temperature, and then stained with anti-mouse CD31 APC (clone 390, ebioscience) and anti-mouse F4/80 Alexa Fluor 488 (clone CI:A3–1, Biolegend) for 60 min in PBS containing 1% goat serum. Tissues were washed 3 times with PBS and 1 time with PBS + DAPI (1/15,000) and mounted in ProLong gold antifade reagent (Invitrogen). Microscopy was performed with Zeiss Axio Imager Z2 with apotome for optical sectioning (courtesy of Dr. K. S. Ravichandran). The fluorescence of AF488/anti-F4/80-stained macrophages, and DAPI-stained cell nuclei on each tissue section was measured by NIH ImageJ 64.

Kupffer Cell Depletion—Tissue macrophages were depleted by one or two injections of intravenous clodronate-containing or control liposomes (0.55 mg of clodronate/10 g; eEncapsula Nano Sciences) given 2 days before, and/or 5 days after starting diets. To prevent an off-target effect of clodronate such as depletion of monocytes, we used a low concentration of clodronate and accessed the frequency of blood and bone marrow monocytes by cytometry.

Liver Cell Preparation—Livers were slowly flushed with PBS via the portal vein, and then perfused with PBS, 0.05% collagenase. The liver was minced and ground on the screen. Cell suspension was further digested with PBS, 0.05% collagenase at 37 °C for 20 min. For mononuclear hepatic leukocytes preparation, cells were prepared as previously described (12). For whole liver cell preparation, cell suspension was further digested with DNase (50 ng/ml). Total liver cells were collected after centrifugation. Red blood cells were removed with ACK lysing buffer. Cells were washed and processed for FACS staining.

RNA Isolation, cDNA Synthesis, and Real-time qPCR Analysis—PBS-perfused liver tissues were snap frozen in nitrogen, and store at −80 °C. Frozen tissues were transferred into RNAlater-ice frozen tissue transition solution (Applied Biosystems) to protect RNA from degradation during thawing. RNA from samples was extracted by the TRIzol (Invitrogen) method following the manufacturer's instructions. RNA integrity and concentration were accessed by a nanodrop spectrophotometer. 250 ng of RNA was treated with DNase I (Invitrogen), and reverse transcribed using the High Capacity RNA to cDNA Master Mix (Applied Biosystems). The real-time quantitative PCR (qPCR) was performed using a Step One Plus Real-time PCR instrument ABI (Applied Biosystems). The levels of *Ccr2*, *Tnfa*, *Ptgs2*, *Timp-1*, and *Hprt* were determined using the TaqMan gene expression assay (Applied Biosystems) and TaqMan gene expression master mix (Applied Biosystems). The relative expression of each gene was calculated using the comparative C_t method normalized to *Hprt* expression. Data are presented as fold-induction of expression compared with the control condition. TaqMan probes used were *Ccr2* (Mm01216173_m1), *Tnfa* (Mm00443258_m1), *Ptgs2* (Mm01307329_m1), *Timp-1* (Mm00441818_m1), and *Hprt* (Mm00446968_m1).

Measurements of Cytokines and Chemokines by Luminex—Mononuclear liver cells were surface stained and sorted for monocytes ($CD45^+CD11b^+NK1.1^-F4/80^{low}CD11b^{int}$ without neutrophils) and resident macrophages ($CD45^+NK1.1^-F4/80^{hi}CD11b^{low}$) with i-Cyt Reflection cell sorters (UVA Flow Cytometry Core Facility). Sorted cells were in overnight cultures with Iscove's modified Dulbecco's medium supplemented with 10% FBS and L-glutamine. Supernatants collected for

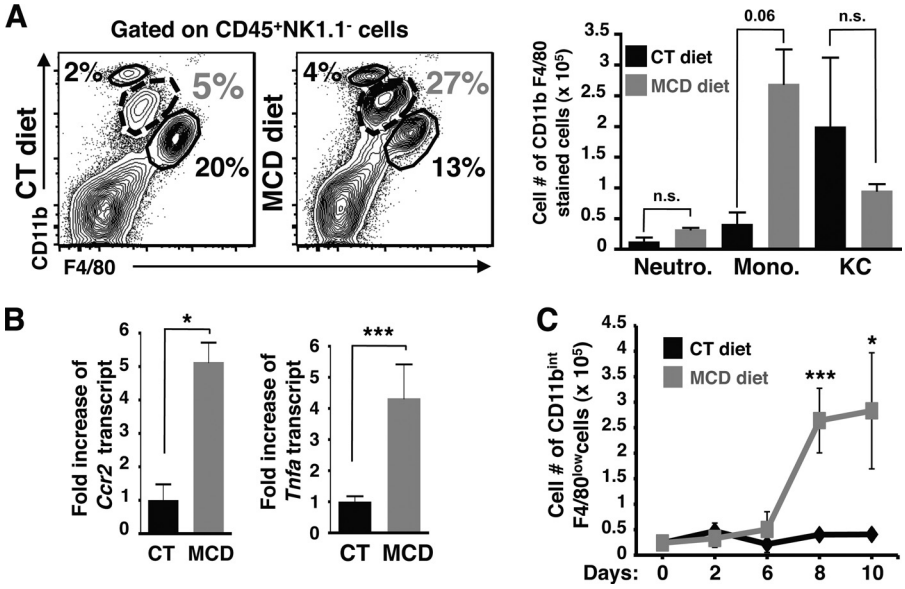

FIGURE 1. **Blood monocytes represent the major source of infiltrated cells after 10 days of NASH-inducing diet.** *A*, the FACS plots and cell numbers of neutrophils ($CD11b^{hi}F4/80^{-}$), monocytes ($CD11b^{int}F4/80^{low}$), and Kupffer cells ($CD11b^{+}F4/80^{hi}$) are shown in $CD45^{+}NK1.1^{-}$-gated whole liver cells isolated from mice fed CT and MCD diets. Representative FACS plots and histograms show an increase in frequency and cell numbers of monocytes. Data are representative of at least four independent experiments with a total of $n = 8$ mice per condition. *B*, hepatic *Ccr2* and *Tnfa* transcript expression was determined by qPCR from whole liver samples of mice fed CT and MCD diets. The RNA level is expressed as fold-induction compared with control diet. Data represent mean ± S.D. *C*, cell number of monocytes within $CD45^{+}NK1.1^{-}$-gated mononuclear liver cell fraction isolated from mice fed CT and MCD diets after 0, 2, 6, 8, and 10 days, with a total of $n = 3$ mice per condition. *, $p < 0.05$ and ***, $p < 0.0005$ as determined by two-tailed *t* test.

multi-plex Millipore assays were performed by UVA Flow Cytometry Core Facility using Luminex 100IS System. Millipore Luminex assays on whole liver tissues were done on liver lysates after homogenization and sonication in ice-cold lysis buffer (PBS, 0.2% Triton X-100, protease inhibitor mixture).

Flow Cytometry and TNFα Intracellular Staining—Liver cells were incubated with a 2.4G2/hamIgG mixture to block Fc receptors, and then with specific antibodies for cell surface staining: CD45 (30F11), NK1.1 (clone PK136), and F4/80 (clone BM8) from eBioscience; CD11b (M1/70), Ly6G (1A8), and Ly6C (AL-21) from BD Biosciences. For TNFα intracellular staining, mononuclear cells were incubated in the presence of GolgiStop (Monensin) at 37 °C, and then washed. After cell surface staining (see above), cells were re-suspended into Cytofix/Cytoperm buffer (BD Biosciences), and stained for intracellular TNFα (MP6-XT22, eBioscience) and isotype control (rat IgG1K). Samples were run on a FACSCanto II and analyzed using FlowJo software. FACS compensations were done with BD Biosciences compensation bead-based single colors according to the manufacture's instructions. Fluorescence minus one were used for setting the gates. The gating strategy is shown in supplemental Fig. S1*A*.

Silencing of TNFα by Specific siRNA Delivered by Lipid Nanoparticles—0.5 mg/kg of siRNA specific to TNFα or luciferase encapsulated in lipid nanoparticles was intravenously injected to mice on day −3, day 0, day +4, and day +7 of diets. Liver tissues were harvested at day 10. The sequence for sense and antisense strands of TNFα siRNAs were previously published (13).

Statistics—The unpaired Student's *t* test (2 tailed) was used for all analysis. $p < 0.05$ was considered statistically significant. *, **, and *** indicate $p < 0.05$, $p < 0.005$, and $p < 0.0005$, respectively.

RESULTS

Inflammatory Monocytes Represent the Major Source of Infiltrated Cells after 10 Days of NASH-inducing Diet—Previous studies have shown an infiltration of inflammatory leukocytes into the liver in murine NASH models after several weeks of diet. To understand the initiation of NASH development such as the early switch of benign steatosis to steatohepatitis, we performed our studies in early stages of NASH disease between 2 and 10 days of feeding. To this end, we characterized the inflammatory leukocytes infiltrated into steatotic livers by performing immune cell phenotyping on whole hepatic cell populations isolated from mice fed with MCD and control diet for 10 days (Fig. 1). Gating strategy to distinguish infiltrating blood monocytes and tissue macrophages are shown in supplemental Fig. S1*A*. Our data show that frequencies (supplemental Fig. S1*B*) and cell numbers of $CD11b^{int}F4/80^{low}$ monocytes within the $CD45^{+}NK1.1^{-}$ liver cell population were increased, whereas Kupffer cells (identified as $CD11b^{low}F4/80^{hi}$ cells) and neutrophils ($CD11b^{hi}F4/80^{-}$) showed no significant cell number difference compared with those from control livers (Fig. 1*A*). On the other hand, the frequencies and cell numbers of liver T ($CD3^{+}$), NKT ($CD3^{+}NK1.1^{+}$), and NK ($CD3^{-}NK1.1^{+}$) cells did not change between mice fed with control and MCD diets (supplemental Fig. S1*C*) during this early phase of NASH disease.

This infiltration of monocytes into livers was confirmed by the increase of *Ccr2* transcript expression in livers isolated from mice fed with a MCD diet compared with control diet (Fig. 1*B*). *Ccr2* transcript encodes the CC-chemokine receptor 2, which is required for infiltration of blood monocytes into inflamed tissues. This increase in CCR2 expression and monocyte infiltration is also associated with an elevated expression of *Tnfa*

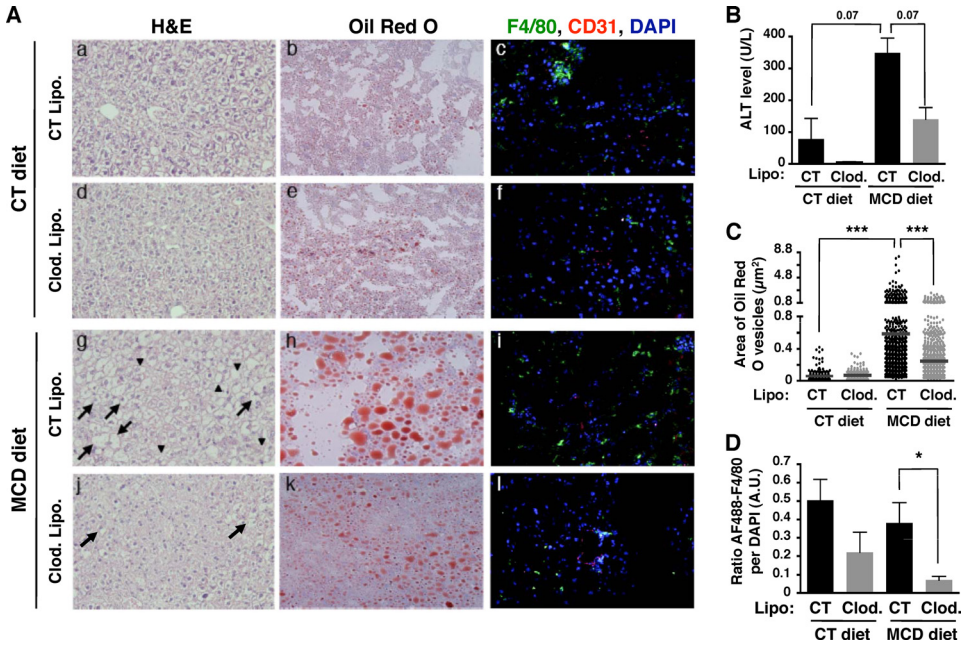

FIGURE 2. **The initiation of NASH disease depends on resident liver macrophages.** *A*, C57BL/6 mice fed CT or MCD diets were treated either with two injections of control liposomes (*CT Lipo.*) or clodronate-containing liposomes (*clod. Lipo.*). H&E-stained (*a*, *d*, *g*, and *j*) and Oil-Red O-stained (*b*, *e*, *h*, and *k*) tissue sections were examined under a bright field microscope at ×200 magnification. Liver sections were also stained with anti-F4/80 (*green*), anti-CD31 (*red*), and DAPI (*blue*), and examined under a apotome fluorescent microscope at ×200 magnification (*c*, *f*, *i*, and *l*). *Arrows* and *arrowheads* indicate ballooning hepatocytes and lipid inclusion, respectively. *B*, serum ALT was measured to assess liver injury. *C*, Oil-Red O staining revealed lipid accumulation in hepatocytes. Area of Oil-Red O-stained vesicles (μm^2) was quantified using Zeiss axiovision software. Counting was done on 2–3 different views on each mouse/treatment group. *D*, macrophage depletion was assessed by the loss of AF488 anti-F4/80 fluorescence. The ratio of green pixel (AF488 anti-F4/80) was normalized to DAPI pixel (cell nucleus) on each tissue section and was measured by NIH ImageJ 64. *, $p < 0.05$ and ***, $p < 0.0005$ as determined by two-tailed *t* test.

(which encodes TNFα, Fig. 1*B*). This monocyte infiltration appears as early as 6 days of MCD diet, continues to increase and accumulate during days 8 and 10 of MCD diet feeding (Fig. 1*C*), and is still observed after 25 days of MCD compared with control diet (data not shown). Other proinflammatory mediators are associated with monocyte infiltration such as *Ptgs2* (encodes for COX-2) and *Timp-1* (tissue inhibitor of metalloproteinase-1) (supplemental Fig. S2*A*); several murine and human studies indicate that Timp-1 has a diagnostic value in detecting early stage of fibrosis (14). In addition, monocyte chemoattractant cytokines such as IP-10 and MCP-1 were increased in whole liver cell lysates from MCD diet-fed mice (supplemental Fig. S2*B*). Taken together, these results indicate that after 10 days of MCD diet, steatotic livers are inflamed with an increase of TNFα expression (among other proinflammatory genes), and enriched in chemokines involved in the recruitment of $CD45^+NK1.1^-CD11b^{int}F4/80^{low}$ monocytes.

Resident Kupffer Cells Trigger the Development of NASH by Promoting Hepatic Lipid Deposition and Inflammation—Resident Kupffer cells play an important role in liver homeostasis, and in mounting local inflammatory responses. To determine a role for liver resident macrophages in the early stages of NASH progression, we depleted resident macrophages by using clodronate-containing liposomes at 2 days before and 5 days after feeding. Depletion of macrophages was confirmed by a decreased numbers of F4/80-positive cells in liver (Fig. 2*A*, *f* and *l* compared with *c* and *i*; and Figs. 2*D* and 3*A*). Histological analysis of livers from MCD diet-fed mice treated with control liposomes showed both an increase in ballooned hepatocytes and intracellular lipid droplets compared with control animals (Fig. 2*A*, *g* and *h* compared with *a* and *b*), as well as increased serum ALT levels (Fig. 2*B*) indicating liver injury. Strikingly, the depletion of macrophages/Kupffer cells showed reduced levels of serum ALT activity (Fig. 2*B*). Clodronate treatment in MCD diet-fed mice also significantly reduced the incidence of ballooned hepatocytes (Fig. 2*A*, *j* compared with *g*) and steatosis (Fig. 2*A*, *k* compared with *h*, and *C*). These data suggest that macrophages might play an important role in inducing lipid deposits in hepatocytes. It also implicates that cross-talk between hepatic lipid accumulation and liver-resident macrophages is likely to be crucial for the progression of simple steatosis to NASH.

A Differential Role for Kupffer Cells and Monocytes during the Early Development of NASH—We next examined whether Kupffer cells initiate inflammatory responses during the MCD diet and contribute to the blood monocyte infiltration. To this end, Kupffer cells were depleted by two injections of clodronate liposomes and their numbers from control- and MCD diet-fed mice were decreased by 38 and 99% compared with respective control mice (Fig. 3*A*, *right panel*). The flow cytometry analysis on hepatic mononuclear cells showed an infiltration of $CD11b^{int}F4/80^{low}$ monocytes in livers of mice MCD-diet-fed treated with control liposomes (Fig. 3*A*, *left panel*), as observed in whole liver cells (Fig. 1*A*). Upon Kupffer cell depletion, we did not detect any increase in the infiltration of blood monocytes. Indeed, the number of monocytes from both MCD and control diet-fed mice treated with clodronate liposomes are similar, and quantitatively equivalent to the number of monocytes from control mice (control diet and control liposomes). Moreover, the depletion of Kupffer cells resulted in abrogation

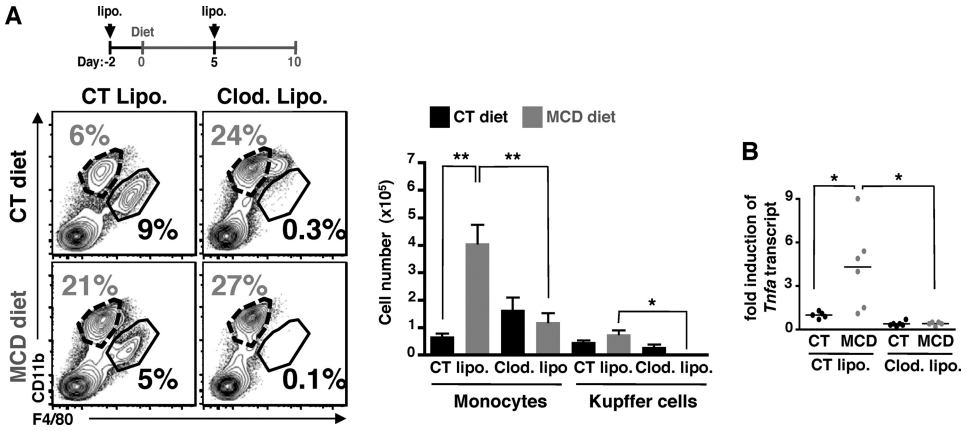

FIGURE 3. **Kupffer cells induce lipid accumulation and monocyte infiltration into the liver.** *A,* C57BL/6 mice fed CT and MCD diets for 10 days were injected twice with control liposomes (*CT Lipo.*) or clodronate-containing liposomes (*clod. Lipo.*) at days −2 and +5 of feeding (see schematic). The representative FACS plots (*left panels*) and cell numbers of monocytes ($CD11b^{int}F4/80^{low}$) and Kupffer cells ($CD11b^{+}F4/80^{hi}$) (*right panel*) are shown in $CD45^{+}NK1.1^{-}$-gated liver mononuclear cells. The neutrophils ($CD11b^{hi}F4/80^{-}$) are gated out of the analysis. Representative FACS plots and compiling data of cell numbers show an increase in frequency and cell numbers of monocytes. Data are from 3 independent experiments with a total of $n = 6$ mice per condition. *B,* hepatic *Tnfa* transcript expression was determined by qPCR from whole liver samples of mice fed CT and MCD diets. The RNA level is expressed as fold-induction compared with control diet. Data represent mean ± S.D. *, $p < 0.05$ and **, $p < 0.005$ as determined by two-tailed *t* test.

of MCD diet-induced hepatic TNFα expression (Fig. 3*B*). It suggests that lack of Kupffer cells during 10 days of feeding abrogates the infiltration of monocytes as well as the induction of steatosis, inflammation, and liver damage.

To address the respective contribution of resident macrophages and infiltrated blood monocytes in NASH development, we sequentially depleted the resident macrophages either 2 days before, or 5 days after feeding (Fig. 4). Of note, the depletion of Kupffer cells is fully achieved after 2 days of one single injection of clodronate liposomes, and the recovery of Kupffer cells is completed after 6 to 7 days post-injection.[3] The depletion of Kupffer cells 2 days before starting 10-day diets slightly decreased the level of serum ALT (Fig. 4*A*) suggesting a possible delay in NASH development, but lipid deposits (Fig. 4*B*) or monocyte infiltration (Fig. 4*C*) into liver were not affected in MCD diet-fed mice. After 10 days of diet, the number of Kupffer cells had returned to the level seen in control mice, suggesting that a pool of Kupffer cells were regenerated during the course of the diet and were still capable of initiating monocyte recruitment and NASH disease. In contrast, the depletion of resident macrophages at 5 days post-diet (and before infiltration of blood monocytes at day 6–7 of MCD diet) showed a decrease in serum ALT level (Fig. 4*D*), lipid accumulation (Fig. 4*E*), and monocyte infiltration (Fig. 4*F*) in livers from MCD diet-fed mice. Moreover, the number of Kupffer cells is still reduced by 65 and 99% compared with respective control mice. Of note, the number and frequency of $CD45^{+}NK^{-}Ly6G^{-}CD11b^{+}Ly6C^{hi}F4/80^{low}$ monocytes from blood and bone marrow were unchanged at day −2 or day +5 of clodronate liposome injections (supplemental Fig. S3, *A* and *B*, respectively). These results suggest that Kupffer cells are the primary cells involved in the initiation of NASH disease, leading subsequently to blood monocyte recruitment into steatotic livers, whereas blood monocytes amplify the ongoing hepatic inflammatory responses.

[3] A.-C. Tosello-Trampont, S. G. Landes, V. Nguyen, T. I. Novobrantseva, and Y. S. Hahn, personal communication.

Kupffer Cells and Blood Monocytes Are Responsible for Mounting Hepatic Inflammatory Responses and Amplifying the Pathogenesis of NASH—To further determine the production of inflammatory mediators by infiltrated monocytes and resident macrophages, we electronically sorted monocytes ($CD45^{+}NK^{-}CD11b^{int}F4/80^{low}$) and Kupffer cells ($CD45^{+}NK^{-}CD11b^{low}F4/80^{hi}$) from MCD and control diet-fed mice; a multiplex luminex assay for chemokines/cytokines was performed on the collected supernatant from *ex vivo* culture of purified monocytes and Kupffer cells (supplemental Fig. S2*C*). Both monocytes and macrophages purified from MCD diet-fed mice were positive for the production of proinflammatory cytokines, TNFα, and several monocytes (IP-10, MCP-1, MIP-2, and MIP-1b) and neutrophil (MIP-1a, RANTES, and KC) chemoattractants.

TNF-α, a key proinflammatory cytokine required for the induction of hepatic inflammation, is secreted by purified Kupffer cells and infiltrated monocytes; we attempted to determine the major cellular source of TNFα production in these myeloid cells before and after monocyte infiltration, after 2 and 10 days of MCD diet. We observed a higher frequency of Kupffer cells ($CD11b^{low}$) positively stained for TNFα than monocytes ($CD11b^{int}$) after 2 days of MCD diet compared with control diet (Fig. 5, *A, right panel*, and *B*). This increase in TNFα production by resident macrophages was observed prior to the infiltration of blood monocytes (Fig. 5*A, left panel*, and *C*), and hepatic inflammation (Fig. 5*E*). Moreover, *ex vivo* culture of sorted Kupffer cells from MCD diet-fed mice indicate that resident macrophages secreted 2-fold more of IL-1α that those from control diet-fed mice (Fig. 5*D*) suggesting they are activated. In contrast, once monocyte infiltration is detectable (Fig. 6*A*, *left panel*), we observed an increased frequency of both Kupffer cells and monocytes stained with TNFα (Fig. 6*A*, *right panel*). Notably, only monocytes showed a higher mean fluorescent intensity (MFI) of TNFα staining (Fig. 6*B*), suggesting that monocytes may produce the highest amount of TNFα during the ongoing progression of NASH development, with Kupffer cells providing a lesser contribution. These results suggest that both Kupffer cells and monocytes con-

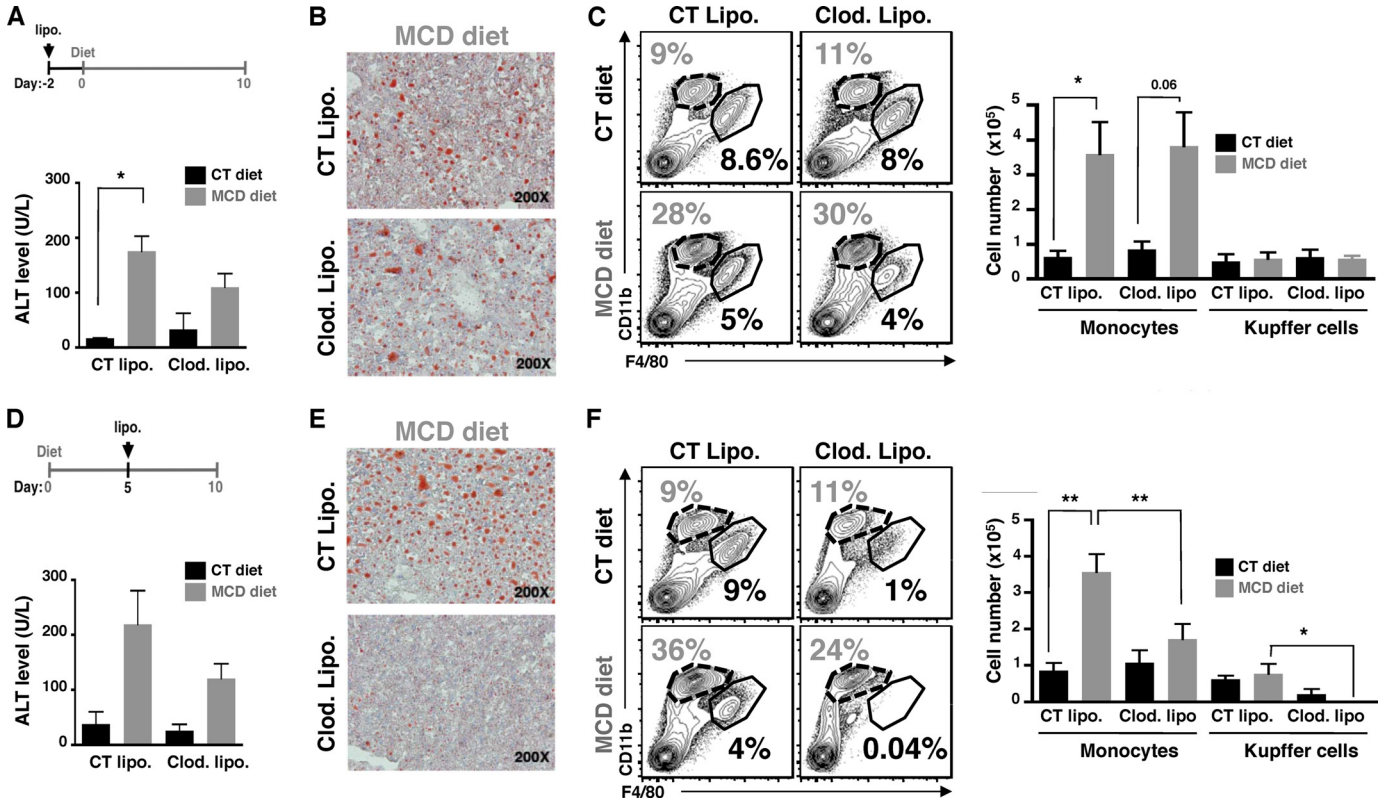

FIGURE 4. **Kupffer cells trigger NASH development by promoting the recruitment of blood monocytes.** C57BL/6 mice fed CT and MCD diets were treated once either with control liposomes (*CT Lipo.*) or clodronate-containing liposomes (*clod. Lipo.*) at 2 days before (*A–C*) or 5 days after (*D–F*) starting feeding (see schematic). *A* and *D,* liver damage is measured by the level of serum ALT. *B* and *E*, hepatic lipid inclusion is determined by Oil-Red O staining on frozen liver sections. *C* and *F*, depletion of infiltrating monocytes ($CD11b^{int}F4/80^{low}$) and Kupffer cells ($CD11b^{+}F4/80^{hi}$) are assessed by the flow cytometry. Data are from 2 independent experiments with a total of $n = 4$ mice per condition. *, $p < 0.05$ and **, $p < 0.005$ as determined by two-tailed *t* test.

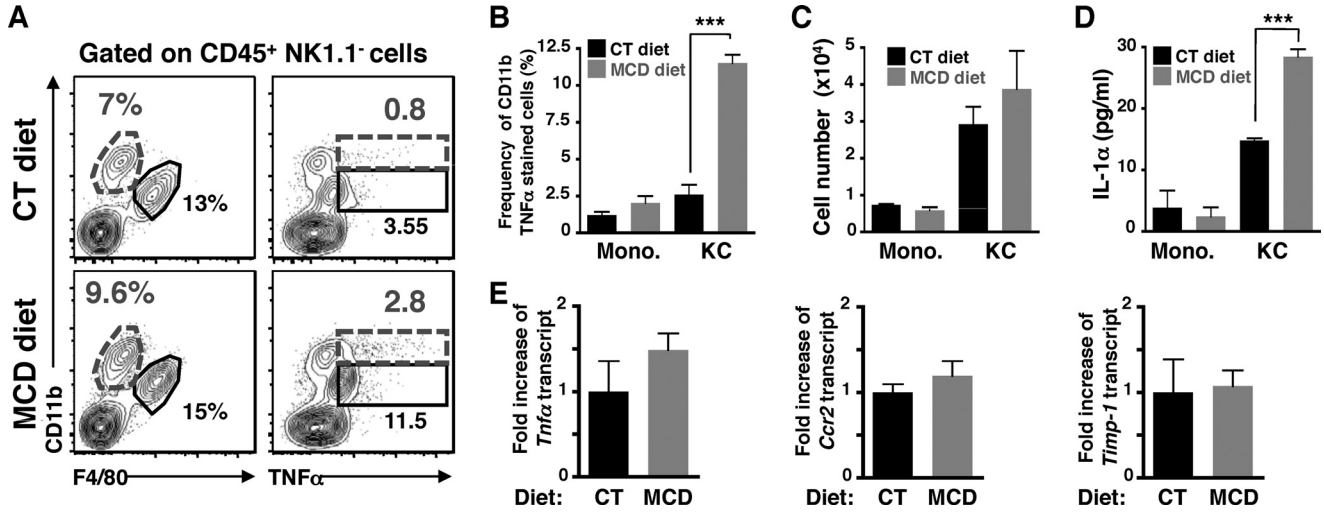

FIGURE 5. **$CD11b^{low}F4/80^{hi}$ Kupffer cells produce TNFα and IL-1α at the early phase of NASH development.** *A*, representative FACS plots of CD11b-stained cells *versus* F4/80 (*left*), or intracellular TNFα (*right*) expression within $CD45^{+}NK1.1^{-}$-gated mononuclear liver cells from mice fed with CT or MCD diets for 2 days. The neutrophils ($CD11b^{hi}F4/80^{-}$) are gated out of the analysis. Monocytes are defined as $CD11b^{int}F4/80^{low}$ cells and Kupffer cells as $CD11b^{low}F4/80^{hi}$. *B*, frequency of $CD11b^{+}$ cells *versus* (*C*) cell number of monocytes ($CD11b^{int}F4/80^{low}$) and Kupffer cells ($CD11b^{low}F4/80^{hi}$) after 2 days of diet. *D*, measurement of secreted IL-1α from *ex vivo* culture of sorted Kupffer cells and monocytes. *E*, hepatic expression of *Tnfa*, *Ccr2*, and *Timp-1* were determined by qPCR from whole liver samples from mice fed CT and MCD diets for 2 days. The RNA level is expressed as fold-induction compared with control diet. These results are compiled data from $n = 3–4$ mice per condition, gated on $CD45^{+}NK1.1^{-}$ liver cells from mice fed CT or MCD diets for 2 days. Data represent mean ± S.D. *, $p < 0.05$ and ***, $p < 0.0005$ as determined by two-tailed *t* test.

tribute to the initiation and progression of NASH with sequential kinetics. To further identify specific monocyte subsets producing TNFα, we examined the expression of Ly6C, a marker for monocytes, and TNFα on a $CD11b^{low/int}F4/80^{+}$ gated population (Fig. 6*C*). The cells with the highest frequency and MFI for TNFα were cells with the highest expression of Ly6C (Fig. 6, *D* and *E*), suggesting that these infiltrated blood monocytes are highly inflammatory ($CD11b^{int}F4/80^{low}TNFα^{hi}Ly6C^{hi}$) (15).

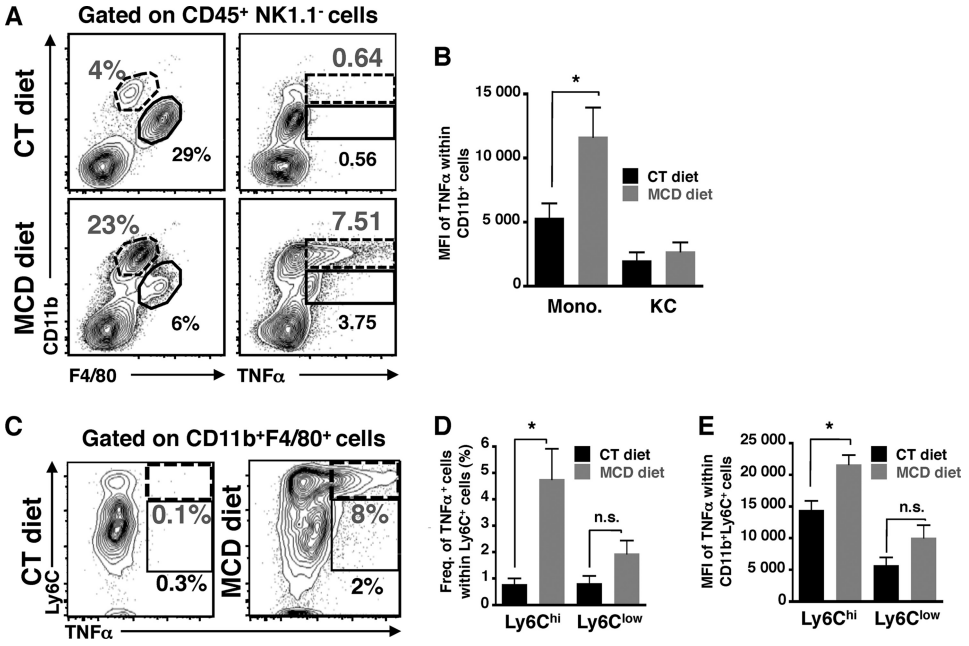

FIGURE 6. **TNFα-producing CD11b^{int}Ly6C^{hi} monocytes are involved in later phase of NASH disease.** *A,* representative FACS plots show CD11b *versus* F4/80 (*left*), or CD11b *versus* intracellular TNFα (*right*) expression in CD45$^+$NK1.1$^-$-gated mononuclear liver cells from mice fed CT and MCD diets for 10 days. *B*, histogram of MFI of TNFα from gated monocytes (CD11b^{int}F4/80^{low}) and Kupffer cells (CD11b^{low}F4/80^{hi}). Representative FACS data of two independent experiments with a total of $n = 4$ mice per condition. *C,* representative FACS plots of TNFα in monocytes (CD11b^{int}F4/80^{low}Ly6C^{hi}) and Kupffer cells (CD11b^{low}F4/80^{hi}Ly6C^{low}) within CD11b$^+$F4/80$^+$CD45$^+$NK1.1$^-$ liver cells. *D*, frequency and *E,* MFI histograms are compiled data from three independent experiments with a total of $n = 4–6$ mice per condition. *, $p < 0.05$ and ***, $p < 0.0005$, as determined by two-tailed *t* test.

Specific Silencing of TNFα in Myeloid Cells Reduces NASH Pathogenesis by Blocking Monocyte Infiltration—To determine whether TNFα produced by myeloid cells was a key component of the initiation of NASH disease, we used siRNAs targeting TNFα encapsulated into lipid nanoparticles formulated to target myeloid cells (tissue macrophages and monocytes) (13). TNFα was efficiently knocked down in whole liver and myeloid cells as, respectively, determined by qPCR (Fig. 7*D*) and FACS analysis (Fig. 8*C*). Histological analysis of liver tissues showed a decrease both in steatosis and in ballooning hepatocytes in TNFα-siRNA, but not in Luc-siRNA-treated mice fed with a MCD diet (Fig. 7*A, h* compared with *f*). The number of Oil Red O-stained vesicles in liver sections (Fig. 7, *A, l* compared with *j*, and *B*) and serum ALT levels were also significantly reduced (Fig. 7*C*) following TNFα silencing in myeloid cells. TNFα silencing targeted to myeloid cells in MCD diet-fed mice decreased the frequency and cell numbers of infiltrated monocytes similar to levels in control mice (Fig. 8, *A* and *B*). Notably, knockdown of TNFα in myeloid cells resulted in decreased expression of Timp-1 (Fig. 8*D*), as well as decreased production of IP-10 and MCP-1 (Fig. 8*E*). Taken together, our data strongly suggest that TNFα-producing myeloid cells such as Kuppfer cells play a key role in the initiation of NASH disease in a murine model.

DISCUSSION

In this report, we demonstrate that hepatic resident macrophages and infiltrated monocytes, respectively, contribute to the initiation and progression of NASH. Although there was no quantitative change in other known infiltrating cell types (such as neutrophils, NK cells, NKT cells, and T cells), we noted a significant influx of blood monocytes into the liver during NASH development. We have shown a differential contribution of Kupffer cells and blood monocytes during the development and progression of NASH. A pre-diet or post-diet depletion of Kupffer cells revealed their role in triggering NASH disease by allowing the recruitment of blood monocytes. Kupffer cells participate as the first innate cells responding to hepatocyte injury due to lipid deposition; as we found that CD11b^{low}F40/80^{hi} Kupffer cells produced IL-1α, and are predominantly stained for TNFα during the early phase (*i.e.* day 2) of NASH development than CD11b^{int}F40/80^{hi} monocytes. These data suggest that Kupffer cells are activated and differentiate toward M1 macrophages. In contrast, CD11b^{int}Ly6C^{hi} monocytes appear to be the predominant source of TNFα production at the later time point (day 10) of MCD diet leading to NASH progression. These infiltrated CD11b^{int}F4/80^{low}TNFα^{hi}Ly6C^{hi} monocytes have potent proinflammatory activity. Importantly, TNFα silencing specifically targeted to myeloid cells reduced the incidence of NASH development through the inhibition of IP-10 and MCP-1 chemokine production. Of note, this is the first report demonstrating that TNFα-mediated MCP-1 and IP-10 production by macrophages/monocytes is crucial for promoting the development and progression of NASH. Our data suggest that both Kupffer cells and infiltrated monocytes have the ability to propagate the lipid accumulation induced by the diet, primarily through production of TNFα. Because Kupffer cells are the first responders to hepatic injury, they may detect the expression of damage-associated molecular patterns expressed on hepatocytes injured by steatosis. The subsequent production of TNFα by Kupffer cells thus propagates the initial insult, leading to inflammation and recruitment of inflammatory monocytes, further accelerating the disease.

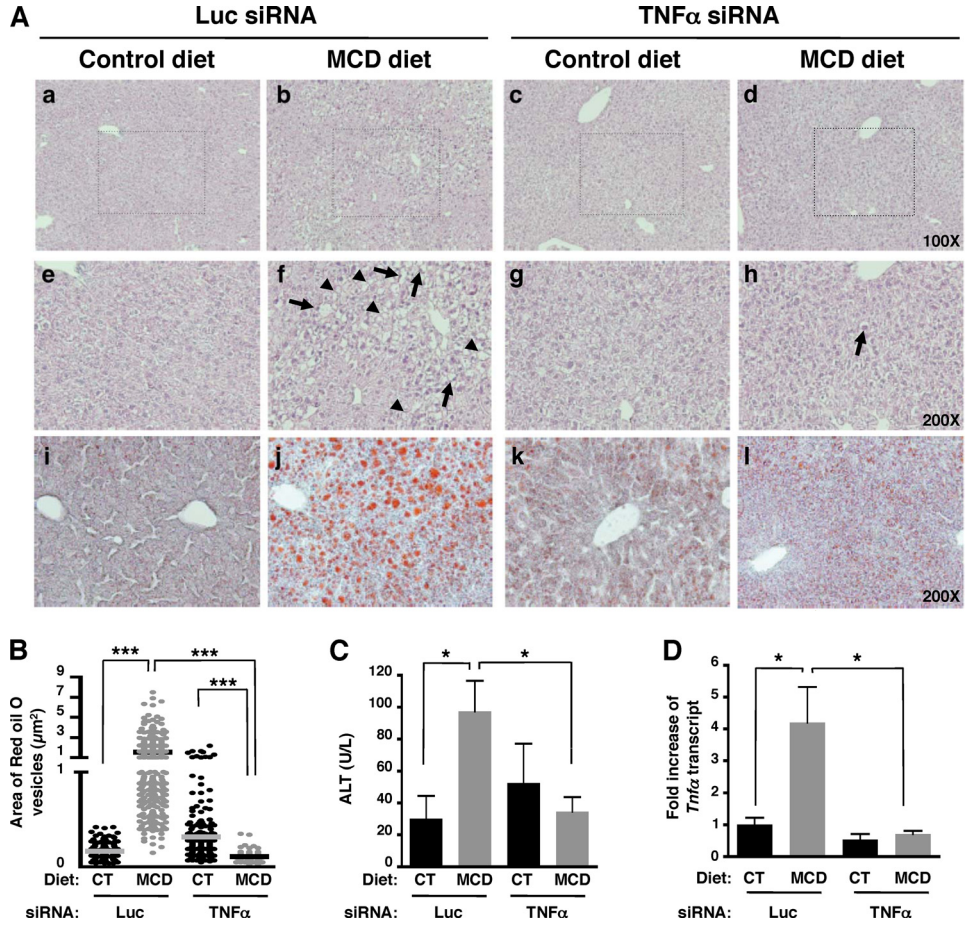

FIGURE 7. **Silencing of TNFα in targeted myeloid cells reduces NASH development.** C57BL/6 mice fed CT and MCD diets were intravenously injected either with control luciferase (*Luc*) or TNFα siRNA liposomes on days −3, 0, 4 and 7. *A*, H&E staining (×100 and 200 magnification) (*a–h*), and Oil-Red O-stained tissue sections (*i–l*) were examined under bright field microscope. Representative images from three independent experiments with a total of $n = 6$ mice per condition. *Arrows* and *arrowheads* indicate ballooning hepatocytes and lipid inclusion, respectively. *B*, area of Oil-Red O-stained vesicles (μm^2) was quantified using zeiss axiovision software. Counting was done on 2–3 different views on each mouse per treatment group. *C*, serum ALT was measured. *D*, silencing of TNFα in targeted myeloid cells abrogated the increased expression of hepatic *Tnfa* transcript. *Tnfa* transcript was determined by qPCR from whole liver samples. *, $p < 0.05$; **, $p < 0.005$; and ***, $p < 0.0005$, as determined by two-tailed *t* test.

The IL-1 family is a group of cytokines that play a key role in regulating immunoinflammatory response. IL-1α and IL-1β are mostly secreted by activated macrophages through inflammasome activation (16), and they stimulate the expression of adhesion molecules on endothelial cells to enhance the transmigration of leukocytes. Kupffer cells promote hepatic steatosis via an IL-1β-dependent mechanism (17). Interestingly, IL-1β enhanced the cytotoxicity effect of TNFα on cultured hepatocytes (18). Our data have shown that Kupffer cells produced IL-1α and TNFα after only 2 days on the MCD diet (Fig. 5, *A*, *B*, and *E*), suggesting that activated Kupffer cells might enhance hepatic lipid accumulation and liver injury through local secretion of IL-1α and TNFα.

The proinflammatory cytokine, TNFα, plays a critical role in the pathogenesis of numerous human diseases. In the liver, tissue macrophages including Kupffer cells and infiltrated monocytes are the primary source of TNFα (19). Our data suggest a cross-talk between macrophages and lipid metabolism through the local production of TNFα. Diverse studies have shown that TNFα can regulate lipid metabolism through a variety of mechanisms depending on the type of cell or tissue (20, 21). In addition to a direct role of TNFα in inducing hepatic steatosis, TNFα is also involved in promoting proinflammatory responses. Activated myeloid cells produce several T-helper-1 cytokines that can amplify the inflammatory response in the liver, leading to further liver damage and hepatic steatosis. This is further supported by our findings that there is an increased intrahepatic expression of MCP-1 and IP-10, which are responsible for the recruitment of inflammatory cells to the liver (supplemental Fig. S2). Based on the finding that the silencing of TNFα in myeloid cells results in a decrease of MCP-1 and IP-10 production (Fig. 8*E*), we propose that TNFα plays a pivotal role in activating myeloid cells and inducing MCP-1 and IP-10 production. Because lipid nanoparticles could also target hepatocytes, we would also expect to efficiently silence TNFα in hepatocytes, if any is produced, by treatment with TNFα-siRNA nanoparticles. However, the depletion of Kupffer cells alone by clodronate liposome treatment resulted in decreased *Tnfa* expression in livers, suggesting that Kupffer cells are responsible for the hepatic expression of TNFα (Fig. 3*B*).

Recently, proinflammatory cytokines such as IL-6 and TNFα have been suggested to regulate the progression from hepatic steatosis to steatohepatitis in obese mice (22). However, other

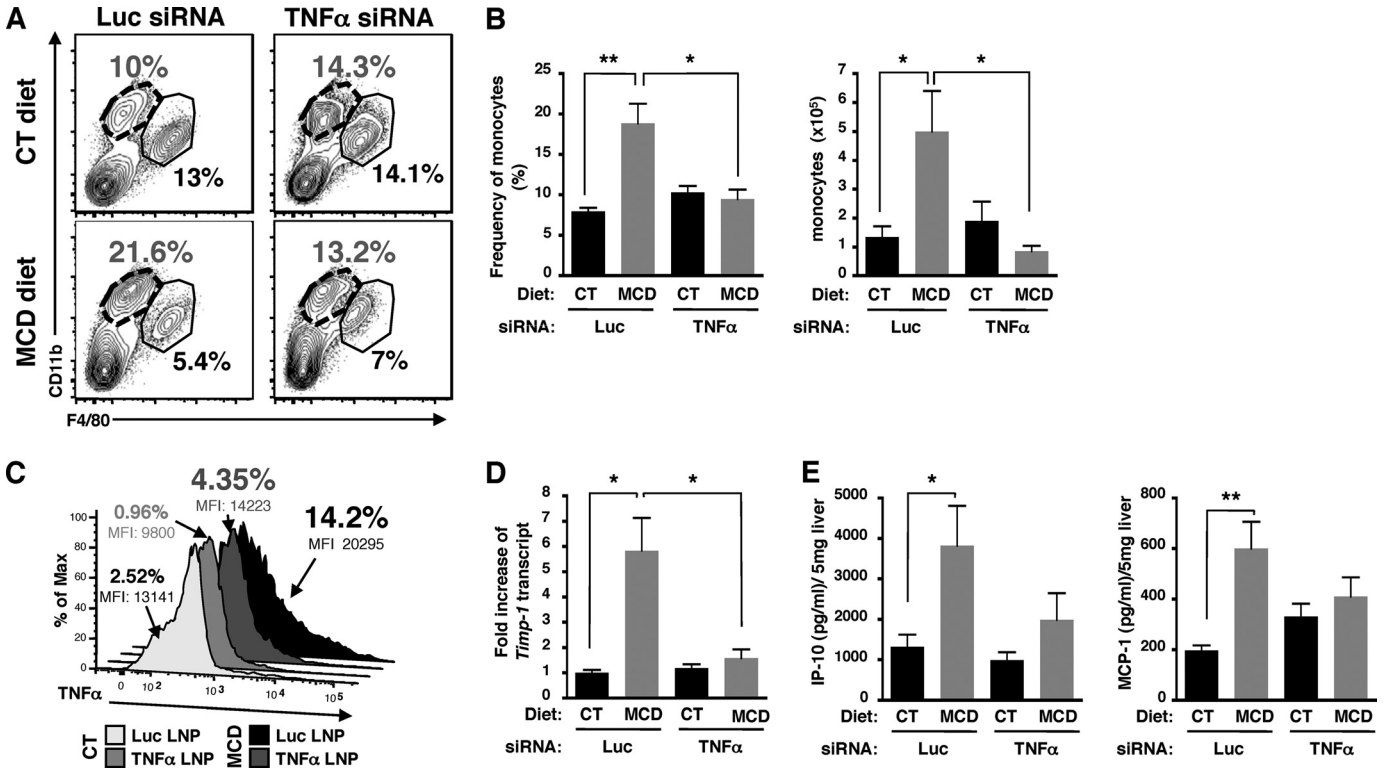

FIGURE 8. **Silencing of TNFα in targeted myeloid cells reduces monocyte infiltration.** *A*, representative FACS plots of CD11b *versus* F4/80 expression within $CD45^+NK1.1^-$-gated mononuclear liver cells isolated from mice fed CT and MCD diets treated with control luciferase (*Luc*) or TNFα siRNA liposomes. The neutrophils ($CD11b^{hi}F4/80^-$) are gated out of our analysis. Representative FACS plots are from a total of $n = 6$ mice per condition. *B*, frequency and cell number of monocytes from three independent experiments with a total of $n = 6$ per condition. *C*, knockdown of TNFα in myeloid cells (Kupffer cells and monocytes). *D*, fold-induction of hepatic *Timp-1* transcript expression determined by qPCR in whole livers. *E*, level of chemokine/cytokine from whole liver cell lysates with a total of $n = 4–6$ mice per condition. Data represent mean ± S.D. *, $p < 0.05$; **, $p < 0.005$; and ***, $p < 0.0005$, as determined by two-tailed *t* test.

studies have shown that IL-6 deficiency or blockade reduced liver inflammation without affecting the development of steatosis suggesting a role for IL-6 only in promoting liver inflammation (11, 23). Furthermore, numerous studies show the contribution of TNFα to NASH development such that NASH patients and murine NASH models exhibit elevated serum levels of TNFα and increased expression of TNFα transcripts in liver and adipose tissues. Although mice lacking TNFα or TNFα receptor type 1 still develop obesity and steatohepatitis (24), studies with TNFα receptor 1- and 2-double deficient mice suggest that TNFα/TNFR-mediated signaling may play a critical role in the pathogenesis of liver fibrosis in murine NASH models (25). Furthermore, hepatic TNFα appears to regulate the activation of Kupffer cells through both a paracrine and autocrine manner (26). Despite numerous studies that have attempted to address the critical role of TNFα in NASH disease, its role as a putative therapeutic target has not yet been elucidated.

Several studies have reported an important pathological role of MCP-1 and IP-10 production in human inflammatory diseases, including liver injury. Notably in HCV infection, the elevated level of IP-10 correlates with necroinflammation (27) and severity of steatosis (28), whereas elevated levels of MCP-1 correlates with more advanced fibrosis (29). In NASH disease, the role of MCP-1 is controversial; MCP-1 deficiency in mice fed a MCD diet does not affect the development of steatohepatitis, but decreases fibrosis (30), or has no effect (31). Recently, pharmacological inhibition of MCP-1 or the lack of CCR2 expression (MCP-1 receptor) in a murine model of NASH have been found to decrease liver inflammation and steatosis without affecting hepatic fibrogenesis (5, 9). The discrepancy of these results could be due to the use of knock-out mice (with possibilities of compensatory mechanisms) *versus* drugs (with potential off-target effects).

It is worthwhile to point out that similar to our findings in the murine model of NASH development, human NASH is manifested by increased levels of proinflammatory cytokines, TNFα, IL-6, and MCP-1 (3, 32). Moreover, TNFα mRNA is highly expressed in NASH patients with severe fibrosis (33). In our experimental mouse model of NASH, we demonstrate that the resident macrophages and blood-derived monocytes are the main cellular source of TNFα. Indeed, the LPS stimulation of whole blood cells from obese patients with NASH increased production of IL-1α and TNFα, suggesting that overproduction of these cytokines by myeloid cells contributes to the progression of liver damage from simple steatosis to NASH (34). In a study examining NASH patients, MCP-1 levels gradually increased with the severity of lipid accumulation and the histological analysis of liver tissues from NASH patients showed an increase in MCP-1 expression, reflecting the infiltration of CCR2 leukocytes. The pathogenic role of TNFα has also been shown in other liver diseases such as chronic hepatitis C (35). In particular, HCV patients infected with genotype 3 of the virus develop severe steatosis (36, 37). Based on the correlation between the degree of inflammation, macrophage activation, and predominance of the Th1 inflammatory cells producer of

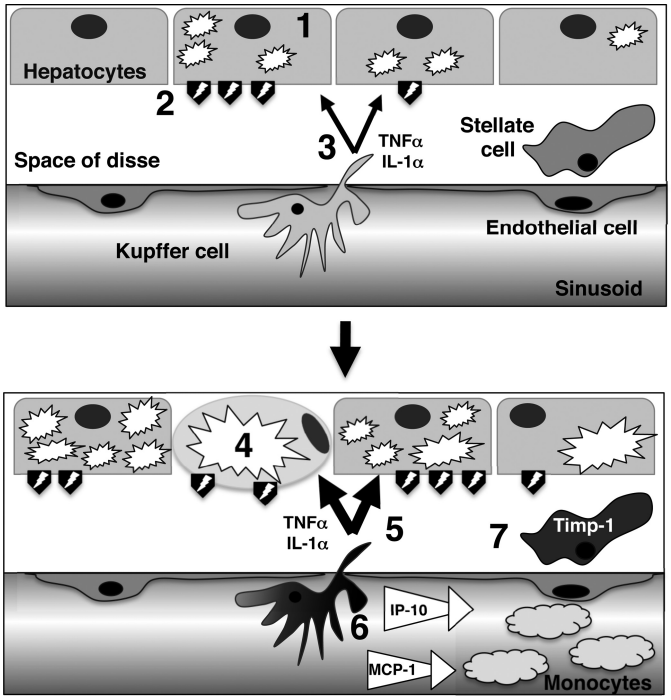

FIGURE 9. **Schematic presentation of the proposed model for the early initiation of NASH development.** See text for details.

TNFα and INFγ in patients with chronic hepatitis C (38, 39), it is possible that HCV might take advantage of the ability of TNFα to regulate lipid metabolism to increase hepatic steatosis. As lipids are essential to the life cycle of HCV (40), an increase in hepatic steatosis might exert a positive effect on virus infection, replication, and propagation. Indeed, the hallmark of liver injury in chronic hepatitis C is elevated hepatic levels of TNFα, INFγ, IP-10, and MCP-1 (41). Moreover, obese patients with HCV develop liver disease more rapidly than lean HCV patients and have higher levels of TNFα, MCP-1, and IP-10 (41). An increase in these cytokines is also associated with the progression to severe liver disease as shown by a higher incidence of hepatocellular carcinoma in HCV patients with NASH (42).

Based on these findings, we propose a pathogenic mechanism of NASH development in mice (Fig. 9): 1) following a metabolic disorder, hepatocytes accumulate lipid vesicles in their cytoplasm; 2) during the initiation stage of NASH disease, injured hepatocytes express or release damage-associated molecular patterns, which would then activate nearby Kupffer cells; 3) the activated Kupffer cells locally produce IL-1α and TNFα; 4) the local production of these cytokines accelerates hepatic steatosis (leading to macrosteatosis) and liver damage by regulating lipid metabolism (inhibition of fatty acid oxidation and increase of serum triglycerides), and hepatic apoptosis; 5) macrosteatosis and hepatic apoptosis/necrosis would further activate Kupffer cells, whereas TNFα stimulates Kupffer cells in an autocrine manner; 6) activated Kupffer cells produce monocyte chemoattractants, which ultimately result in the recruitment of proinflammatory blood monocytes, and amplify the inflammatory response; 7) TNFα directly induces Timp-1 expression in stellate cells, which protects them from apoptosis and leads to the development of fibrosis.

Therefore, it is tempting to speculate that IL-1α and TNFα-producing Kupffer cells are the initiating cells for NASH development that further accelerate lipid accumulation within steatotic hepatocytes and promote progression from simple steatosis to steatohepatitis. During the acute phase response in hepatic infection, inflammation, injury, or stress, TNFα and IL-1 have been shown to alter lipid metabolism (as hypertriglyceridemia and decreased hepatic fatty acid oxidation) by decreasing the expression and/or activity of proteins involved in lipid and lipoprotein metabolism, such as peroxisome proliferator-activated receptor α, retinoid X receptor, and liver X receptor (17, 43). Moreover, TNFα has been revealed as an important regulator of lipid metabolism in different tissues (20). In the liver, TNFα promotes steatosis by increasing fatty acid synthesis through enhanced expression of sterol regulatory element binding protein-1c (SREBP-1c) (44, 45) and suppressing β-oxidation through inhibition of peroxisomal fatty acyl-CoA oxidase (46). TNFα also enhances steatosis by inducing fatty acid uptake and reducing lipid export (47). Furthermore, during NASH development, the expression of the fibrosis marker, hepatic Timp-1, is increased (supplemental Fig. S2*A*), and its expression is abolished following silencing of TNFα in myeloid cells (Fig. 8*D*). Under *in vitro* conditions, TNFα directly induces *Timp-1* expression in stellate cells (25). During hepatic fibrogenesis, stellate cells increase Timp-1 expression that protects them from apoptosis (48). In our model, TNFα-induced Timp-1 might also have antiapoptotic effects on activated stellate cells leading to hepatic fibrogenesis.

There is currently no established medical treatment for NASH patients. Anti-TNFα therapy is often used to treat patients with autoimmune disorders associated with TNFα (49). The use of anti-TNFα-based therapy in patients presenting with both autoimmune and NASH disease has provided some promising results (50). However, anti-TNFα therapy can have severe side effects (49). Therefore, therapeutic intervention by inhibiting TNFα in a specific cell type may help reduce the risk of side effects caused by the prolonged presence of monoclonal antibodies or anti-TNFα blockers. Our studies revealed a potential therapeutic benefit of silencing TNFα in myeloid cells in a transient manner. The silencing of TNFα in myeloid cells strongly prevents steatosis, the production of monocyte chemoattractants (MCP-1 and IP-10), the recruitment of blood monocytes into the liver, and expression of the *Timp-1* gene. Previous studies have shown the beneficial effects of therapeutic siRNA silencing in inflammatory myeloid cells in mouse models of human diseases (13, 51). Thus, the silencing of TNFα in myeloid cells might be a tenable therapeutic approach to reduce the incidence of steatohepatitis.

In summary, our findings suggest that TNFα produced by intrahepatic Kupffer cells can trigger the development of NASH through the enhanced production of IP-10 and MCP-1. In addition, silencing of TNFα in myeloid cells abrogated the production of these chemokines and prevented the development of NASH. Therefore, blockade of TNFα might represent a novel therapeutic target in NASH with the potential to limit tissue injury and possibly prevent the progression to severe liver disease.

Acknowledgments—We thank the University of Virginia Flow Cytometry Core facility for excellent technical assistance with cell sorting and luminex assays. We thank Drs. K. Ravichandran and T. J. Braciale for apotome microscope and one-step-plus qPCR access, respectively. We thank Drs. J. Kinchen and P. Trampont for their technical expertise. We thank Alnylam siRNA synthesis, screening, and formulation groups for providing efficacious reagents. We thank members of Dr. Y. Hahn's laboratory, particularly Dr. M. Lassen, for their suggestions.

REFERENCES

1. Cheung, O., and Sanyal, A. J. (2010) Recent advances in nonalcoholic fatty liver disease. *Curr. Opin. Gastroenterol.* **26,** 202–208
2. Tilg, H., and Moschen, A. R. (2010) Evolution of inflammation in nonalcoholic fatty liver disease. The multiple parallel hits hypothesis. *Hepatology* **52,** 1836–1846
3. Haukeland, J. W., Damås, J. K., Konopski, Z., Løberg, E. M., Haaland, T., Goverud, I., Torjesen, P. A., Birkeland, K., Bjøro, K., and Aukrust, P. (2006) Systemic inflammation in nonalcoholic fatty liver disease is characterized by elevated levels of CCL2. *J. Hepatol.* **44,** 1167–1174
4. Rull, A., Rodríguez, F., Aragonès, G., Marsillach, J., Beltrán, R., Alonso-Villaverde, C., Camps, J., and Joven, J. (2009) Hepatic monocyte chemoattractant protein-1 is up-regulated by dietary cholesterol and contributes to liver steatosis. *Cytokine* **48,** 273–279
5. Miura, K., Yang, L., van Rooijen, N., Ohnishi, H., and Seki, E. (2012) Hepatic recruitment of macrophages promotes nonalcoholic steatohepatitis through CCR2. *Am. J. Physiol. Gastrointest. Liver Physiol.* **302,** G1310–1321
6. Obstfeld, A. E., Sugaru, E., Thearle, M., Francisco, A. M., Gayet, C., Ginsberg, H. N., Ables, E. V., and Ferrante, A. W., Jr. (2010) C-C chemokine receptor 2 (CCR2) regulates the hepatic recruitment of myeloid cells that promote obesity-induced hepatic steatosis. *Diabetes* **59,** 916–925
7. Weisberg, S. P., Hunter, D., Huber, R., Lemieux, J., Slaymaker, S., Vaddi, K., Charo, I., Leibel, R. L., and Ferrante, A. W., Jr. (2006) CCR2 modulates inflammatory and metabolic effects of high-fat feeding. *J. Clin. Invest.* **116,** 115–124
8. Larter, C. Z., and Yeh, M. M. (2008) Animal models of NASH. Getting both pathology and metabolic context right. *J. Gastroenterol. Hepatol.* **23,** 1635–1648
9. Baeck, C., Wehr, A., Karlmark, K. R., Heymann, F., Vucur, M., Gassler, N., Huss, S., Klussmann, S., Eulberg, D., Luedde, T., Trautwein, C., and Tacke, F. (2012) Pharmacological inhibition of the chemokine CCL2 (MCP-1) diminishes liver macrophage infiltration and steatohepatitis in chronic hepatic injury. *Gut* **61,** 416–426
10. Miura, K., Kodama, Y., Inokuchi, S., Schnabl, B., Aoyama, T., Ohnishi, H., Olefsky, J. M., Brenner, D. A., and Seki, E. (2010) Toll-like receptor 9 promotes steatohepatitis by induction of interleukin-1β in mice. *Gastroenterology* **139,** 323–334.e7
11. Mas, E., Danjoux, M., Garcia, V., Carpentier, S., Ségui, B., and Levade, T. (2009) IL-6 deficiency attenuates murine diet-induced non-alcoholic steatohepatitis. *PLoS One* **4,** e7929
12. Lassen, M. G., Lukens, J. R., Dolina, J. S., Brown, M. G., and Hahn, Y. S. (2010) Intrahepatic IL-10 maintains NKG2A$^+$Ly49$^-$ liver NK cells in a functionally hyporesponsive state. *J. Immunol.* **184,** 2693–2701
13. Novobrantseva, T. I., Borodovsky, A., Wong, J., Klebanov, B., Zafari, M., Yucius, K., Querbes, W., Ge, P., Ruda, V., Milstein, S., Speciner, L., Duncan, R., Barros, S., Basha, G., Cullis, P., Akinc, A., Donahoe, J. S., Jayaprakash, K. N., Jayaraman, M., Bogorad, R. L., Love, K., Whitehead, K., Levins, C., Manoharan, M., Swirski, F. K., Weissleder, R., Langer, R., Anderson, D. G., de Fougerolles, A., Nahrendorf, M., and Koteliansky, V. (2012) Systemic RNA1-mediated gene silencing in nonhuman primate and rodent myeloid cells. *Mol. Therapy Nucleic Acids* **1,** e4
14. Boeker, K. H., Haberkorn, C. I., Michels, D., Flemming, P., Manns, M. P., and Lichtinghagen, R. (2002) Diagnostic potential of circulating TIMP-1 and MMP-2 as markers of liver fibrosis in patients with chronic hepatitis C. *Clin. Chim. Acta* **316,** 71–81
15. Shi, C., and Pamer, E. G. (2011) Monocyte recruitment during infection and inflammation. *Nat. Rev. Immunol.* **11,** 762–774
16. Szabo, G., and Csak, T. (2012) Inflammasomes in liver diseases. *J. Hepatol.* **57,** 642–654
17. Stienstra, R., Saudale, F., Duval, C., Keshtkar, S., Groener, J. E., van Rooijen, N., Staels, B., Kersten, S., and Müller, M. (2010) Kupffer cells promote hepatic steatosis via interleukin-1beta-dependent suppression of peroxisome proliferator-activated receptor α activity. *Hepatology* **51,** 511–522
18. Petrasek, J., Dolganiuc, A., Csak, T., Kurt-Jones, E. A., and Szabo, G. (2011) Type I interferons protect from Toll-like receptor 9-associated liver injury and regulate IL-1 receptor antagonist in mice. *Gastroenterology* **140,** 697–708.e4
19. Su, G. L. (2002) Lipopolysaccharides in liver injury: molecular mechanisms of Kupffer cell activation. *Am. J. Physiol. Gastrointest. Liver Physiol.* **283,** G256-G265
20. Chen, X., Xun, K., Chen, L., and Wang, Y. (2009) TNF-α, a potent lipid metabolism regulator. *Cell Biochem. Funct.* **27,** 407–416
21. Im, S. S., Yousef, L., Blaschitz, C., Liu, J. Z., Edwards, R. A., Young, S. G., Raffatellu, M., and Osborne, T. F. (2011) Linking lipid metabolism to the innate immune response in macrophages through sterol regulatory element binding protein-1a. *Cell Metab.* **13,** 540–549
22. Park, E. J., Lee, J. H., Yu, G. Y., He, G., Ali, S. R., Holzer, R. G., Osterreicher, C. H., Takahashi, H., and Karin, M. (2010) Dietary and genetic obesity promote liver inflammation and tumorigenesis by enhancing IL-6 and TNF expression. *Cell* **140,** 197–208
23. Yamaguchi, K., Itoh, Y., Yokomizo, C., Nishimura, T., Niimi, T., Fujii, H., Okanoue, T., and Yoshikawa, T. (2010) Blockade of interleukin-6 signaling enhances hepatic steatosis but improves liver injury in methionine choline-deficient diet-fed mice. *Lab. Invest.* **90,** 1169–1178
24. Dela Peña, A., Leclercq, I., Field, J., George, J., Jones, B., and Farrell, G. (2005) NF-κB activation, rather than TNF, mediates hepatic inflammation in a murine dietary model of steatohepatitis, *Gastroenterology* **129,** 1663–1674
25. Tomita, K., Tamiya, G., Ando, S., Ohsumi, K., Chiyo, T., Mizutani, A., Kitamura, N., Toda, K., Kaneko, T., Horie, Y., Han, J. Y., Kato, S., Shimoda, M., Oike, Y., Tomizawa, M., Makino, S., Ohkura, T., Saito, H., Kumagai, N., Nagata, H., Ishii, H., and Hibi, T. (2006) Tumour necrosis factor alpha signalling through activation of Kupffer cells plays an essential role in liver fibrosis of non-alcoholic steatohepatitis in mice. *Gut* **55,** 415–424
26. Kitamura, K., Nakamoto, Y., Akiyama, M., Fujii, C., Kondo, T., Kobayashi, K., Kaneko, S., and Mukaida, N. (2002) Pathogenic roles of tumor necrosis factor receptor p55-mediated signals in dimethyl nitrosamine-induced murine liver fibrosis. *Lab. Investig.* **82,** 571–583
27. Harvey, C. E., Post, J. J., Palladinetti, P., Freeman, A. J., Ffrench, R. A., Kumar, R. K., Marinos, G., and Lloyd, A. R. (2003) Expression of the chemokine IP-10 (CXCL10) by hepatocytes in chronic hepatitis C virus infection correlates with histological severity and lobular inflammation. *J. Leukocyte Biol.* **74,** 360–369
28. Romero, A. I., Lagging, M., Westin, J., Dhillon, A. P., Dustin, L. B., Pawlotsky, J. M., Neumann, A. U., Ferrari, C., Missale, G., Haagmans, B. L., Schalm, S. W., Zeuzem, S., Negro, F., Verheij-Hart, E., and Hellstrand, K. (2006) Interferon (IFN)-γ-inducible protein-10. Association with histological results, viral kinetics, and outcome during treatment with pegylated IFN-α2a and ribavirin for chronic hepatitis C virus infection. *J. Infect. Dis.* **194,** 895–903
29. Mühlbauer, M., Bosserhoff, A. K., Hartmann, A., Thasler, W. E., Weiss, T. S., Herfarth, H., Lock, G., Schölmerich, J., and Hellerbrand, C. (2003) A novel MCP-1 gene polymorphism is associated with hepatic MCP-1 expression and severity of HCV-related liver disease. *Gastroenterology* **125,** 1085–1093
30. Kassel, K. M., Guo, G. L., Tawfik, O., and Luyendyk, J. P. (2010) Monocyte chemoattractant protein-1 deficiency does not affect steatosis or inflammation in livers of mice fed a methionine-choline-deficient diet. *Lab. Investig.* **90,** 1794–1804
31. Galastri, S., Zamara, E., Milani, S., Novo, E., Provenzano, A., Delogu, W., Vizzutti, F., Sutti, S., Locatelli, I., Navari, N., Vivoli, E., Caligiuri, A., Pinzani, M., Albano, E., Parola, M., and Marra, F. (2012) Lack of CC chemo-

kine ligand 2 differentially affects inflammation and fibrosis according to the genetic background in a murine model of steatohepatitis. *Clin. Sci.* **123,** 459–471
32. Abiru, S., Migita, K., Maeda, Y., Daikoku, M., Ito, M., Ohata, K., Nagaoka, S., Matsumoto, T., Takii, Y., Kusumoto, K., Nakamura, M., Komori, A., Yano, K., Yatsuhashi, H., Eguchi, K., and Ishibashi, H. (2006) Serum cytokine and soluble cytokine receptor levels in patients with non-alcoholic steatohepatitis. *Liver Int.* **26,** 39–45
33. Crespo, J., Cayón, A., Fernández-Gil, P., Hernández-Guerra, M., Mayorga, M., Domínguez-Díez, A., Fernández-Escalante, J. C., and Pons-Romero, F. (2001) Gene expression of tumor necrosis factor α and TNF-receptors, p55 and p75, in nonalcoholic steatohepatitis patients. *Hepatology* **34,** 1158–1163
34. Poniachik, J., Csendes, A., Díaz, J. C., Rojas, J., Burdiles, P., Maluenda, F., Smok, G., Rodrigo, R., and Videla, L. A. (2006) Increased production of IL-1α and TNF-α in lipopolysaccharide-stimulated blood from obese patients with non-alcoholic fatty liver disease. *Cytokine* **33,** 252–257
35. Tilg, H., Wilmer, A., Vogel, W., Herold, M., Nölchen, B., Judmaier, G., and Huber, C. (1992) Serum levels of cytokines in chronic liver diseases. *Gastroenterology* **103,** 264–274
36. Castera, L., Chouteau, P., Hezode, C., Zafrani, E. S., Dhumeaux, D., and Pawlotsky, J. M. (2005) Hepatitis C virus-induced hepatocellular steatosis. *Am. J. Gastroenterol.* **100,** 711–715
37. Bedossa, P., Moucari, R., Chelbi, E., Asselah, T., Paradis, V., Vidaud, M., Cazals-Hatem, D., Boyer, N., Valla, D., and Marcellin, P. (2007) Evidence for a role of nonalcoholic steatohepatitis in hepatitis C. A prospective study. *Hepatology* **46,** 380–387
38. McCaughan, G. W., and George, J. (2004) Fibrosis progression in chronic hepatitis C virus infection. *Gut* **53,** 318–321
39. Napoli, J., Bishop, G. A., McGuinness, P. H., Painter, D. M., and McCaughan, G. W. (1996) Progressive liver injury in chronic hepatitis C infection correlates with increased intrahepatic expression of Th1-associated cytokines. *Hepatology* **24,** 759–765
40. Negro, F. (2010) Abnormalities of lipid metabolism in hepatitis C virus infection. *Gut* **59,** 1279–1287
41. Palmer, C., Corpuz, T., Guirguis, M., O'Toole, S., Yan, K., Bu, Y., Jorgenson, J., Talbot, M., Loi, K., Lloyd, A., and Zekry, A. (2010) The effect of obesity on intrahepatic cytokine and chemokine expression in chronic hepatitis C infection. *Gut* **59,** 397–404
42. Koike, K., and Moriya, K. (2005) Metabolic aspects of hepatitis C viral infection. Steatohepatitis resembling but distinct from NASH. *J. Gastroenterol.* **40,** 329–336
43. Kim, M. S., Sweeney, T. R., Shigenaga, J. K., Chui, L. G., Moser, A., Grunfeld, C., and Feingold, K. R. (2007) Tumor necrosis factor and interleukin 1 decrease RXRα, PPARα, PPARγ, LXRα, and the coactivators SRC-1, PGC-1α, and PGC-1β in liver cells. *Metabolism* **56,** 267–279
44. Endo, M., Masaki, T., Seike, M., and Yoshimatsu, H. (2007) TNF-α induces hepatic steatosis in mice by enhancing gene expression of sterol regulatory element binding protein-1c (SREBP-1c). *Exp. Biol. Med.* **232,** 614–621
45. Pandey, A. K., Munjal, N., and Datta, M. (2010) Gene expression profiling and network analysis reveals lipid and steroid metabolism to be the most favored by TNFα in HepG2 cells. *PLoS One* **5,** e9063
46. Beier, K., Völkl, A., and Fahimi, H. D. (1992) Suppression of peroxisomal lipid β-oxidation enzymes of TNF-α. *FEBS Lett.* **310,** 273–276
47. Yamauchi, T., Kamon, J., Waki, H., Terauchi, Y., Kubota, N., Hara, K., Mori, Y., Ide, T., Murakami, K., Tsuboyama-Kasaoka, N., Ezaki, O., Akanuma, Y., Gavrilova, O., Vinson, C., Reitman, M. L., Kagechika, H., Shudo, K., Yoda, M., Nakano, Y., Tobe, K., Nagai, R., Kimura, S., Tomita, M., Froguel, P., and Kadowaki, T. (2001) The fat-derived hormone adiponectin reverses insulin resistance associated with both lipoatrophy and obesity. *Nat. Med.* **7,** 941–946
48. Yoshiji, H., Kuriyama, S., Yoshii, J., Ikenaka, Y., Noguchi, R., Nakatani, T., Tsujinoue, H., Yanase, K., Namisaki, T., Imazu, H., and Fukui, H. (2002) Tissue inhibitor of metalloproteinases-1 attenuates spontaneous liver fibrosis resolution in the transgenic mouse. *Hepatology* **36,** 850–860
49. Nash, P. T., and Florin, T. H. (2005) Tumour necrosis factor inhibitors. *Med. J. Aust.* **183,** 205–208
50. Li, W., Zheng, L., Sheng, C., Cheng, X., Qing, L., and Qu, S. (2011) Systematic review on the treatment of pentoxifylline in patients with nonalcoholic fatty liver disease. *Lipids Health Dis.* **10,** 49
51. Leuschner, F., Dutta, P., Gorbatov, R., Novobrantseva, T. I., Donahoe, J. S., Courties, G., Lee, K. M., Kim, J. I., Markmann, J. F., Marinelli, B., Panizzi, P., Lee, W. W., Iwamoto, Y., Milstein, S., Epstein-Barash, H., Cantley, W., Wong, J., Cortez-Retamozo, V., Newton, A., Love, K., Libby, P., Pittet, M. J., Swirski, F. K., Koteliansky, V., Langer, R., Weissleder, R., Anderson, D. G., and Nahrendorf, M. (2011) Therapeutic siRNA silencing in inflammatory monocytes in mice. *Nat. Biotechnol.* **29,** 1005–1010